Nonlinear instability of a fluid layer flowing down a vertical wall under imposed time-periodic perturbations

L. A. Dávalos-Orozco
Instituto de Investigaciones en Materiales, Universidad Nacional Autónoma de México, Apartado Postal 70-360, Coyoacán, 04510 México, Distrito Federal, Mexico

S. H. Davis
Department of Engineering Sciences and Applied Mathematics, Northwestern University, Evanston, Illinois 60208

S. G. Bankoff
Department of Chemical Engineering, Northwestern University, Evanston, Illinois 60208
(Received 5 April 1966; revised manuscript received 26 September 1996)

We investigate the nonlinear instability of a fluid layer flowing down a vertical wall and subjected to a continuously imposed oscillatory pressure gradient. In each case the frequency ω of oscillation is fixed. The flow instability is investigated numerically by means of the Benney equation with a space- and time-dependent inhomogeneous term. The wave evolution is followed in space and time for different Reynolds numbers. It is found that for a range of wave numbers near critical, saturation occurs only for frequencies ω smaller than a critical value. For larger frequencies, the waves grow unboundedly everywhere. For ω smaller than that value, subharmonics occur between the curves of criticality and subcriticality. An increase in Reynolds number leads the instability to the region of subcriticality where wave subharmonics appear for all the frequencies investigated in this paper. Larger Reynolds numbers give additional subharmonics until a magnitude is reached, at which the flow becomes chaotic. As the frequency increases above a critical value, subharmonics are more difficult to find in the supercritical region. [S1063-651X(97)06701-9]

PACS number(s): 47.20.Ky, 47.35.+i, 47.52.+j

I. INTRODUCTION

The flow in liquid layers down walls has many industrial applications and has intrinsic complex behavior that is a challenge to describe. Direct numerical simulation of the unsteady Navier-Stokes equations to analyze the thin-film dynamics [1,2] is costly, but the results can be used as a benchmark for other approaches. In the temporal theory Joo and Davis [3] showed via the Benney equation that all equilibrated two-dimensional finite-amplitude waves on a vertical plate are unstable to three-dimensional disturbances.

Some restrictions are important to simplify the governing equations. The long-wavelength assumption by means of a small parameter ϵ is one of them, which implicitly says that the surface slope everywhere is small. When this restriction is no longer satisfied, the integration of the evolution equation must be stopped. Other restrictions are that the Reynolds number G is of unit order and the surface tension σ is large. The applicability of these restrictions has been considered by Frenkel [4].

Benney [5], as well as those who followed (e.g., Gjevik [6], Nakaya [7], Krishna and Lin [8], Pumir *et al.* [9], Chang [10], Nakaya [11], Joo *et al.* [12,13], and Joo and Davis [3,14], and Frenkel [4]), derived a strongly nonlinear equation valid for $\epsilon \to 0$, $\epsilon G = O(\epsilon)$, and $\sigma = O(\epsilon^{-2})$. This equation has been used frequently as a device for studying these surface wave instabilities or coupled to other instabilities due to thermocapillarity, evaporation, etc. (see e.g., [12,15]).

When the Benney equation in two dimensions has been integrated on spatially periodic domains, two ranges of wave number k and G are found: one corresponds to supercritical bifurcations that give saturation and hence permanent finite-amplitude structures and the other corresponds to subcritical bifurcation and unlimited (nonsaturated) growth of disturbances. In the latter case there appears to be blowup under certain conditions in a finite time, indicating that the assumption of small surface slopes is no longer valid. This illustrates the danger in extrapolating the evolution equation solutions beyond their limits of validity. However, Krisnamoorthy *et al.* [2] find that there is quantitative agreement with direct numerical simulations in such cases when G is smaller than 4 or 5, a range of importance to studies of thin-film breakup and dryout [15]. When G is larger, such quantitative agreement is lost.

Sivashisky and Michelson [16] showed that in the weakly nonlinear limit the Benney equation reduces to the Kuramoto-Sivashinsky (KS) equation, which displays no blowup but whose surface amplitude is restricted to a small

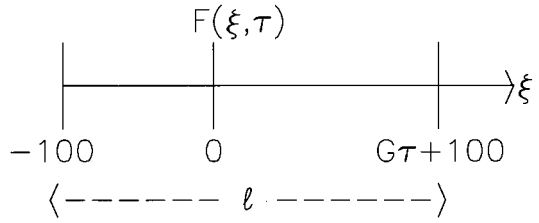

FIG. 1. Sketch of the spatial interval used in the numerical analysis of Eqs. (4) and (9). $F(\xi,\tau)$ is applied locally around the origin. In this paper it has a bell shape with a maximum at the origin, which oscillates in time.

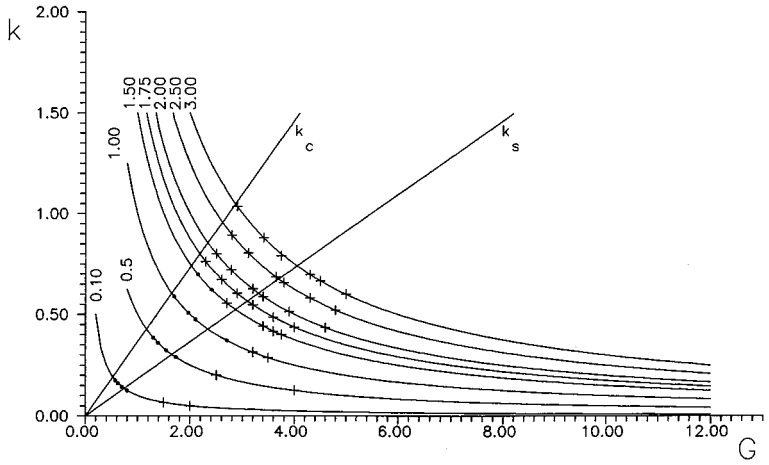

FIG. 2. Graph of k vs G for different frequencies ω. k_c is the critical wave number for linear instability and k_s is the transition value separating supercritical and subcritical bifurcations as found by Gjevik [6]. The supercritical region is between the line of k_c and k_s. The subcritical region is below the line k_s. Dots and crosses denote regions of equilibration and blowup in our spatial theory, respectively.

fraction of the mean film thickness. Thus the Benney equation, where it is valid, can give information unavailable from the KS theory.

If one wishes to describe only quantitatively waves at Reynolds numbers where many experiments on complex dynamics are examined, say, $20<G<100$, one must include inertia at leading order. This can be done approximately using Karman-Pohlhausen methods (see e.g., [17–19]). With lubrication theory assumptions it has been found that all disturbances that grow are convectively unstable [3]. This has been verified experimentally for larger Reynolds numbers by Liu and Gollub [20] for plates of small inclination to the horizontal. The implication of this property is that the system should be analyzed via a spatial-growth theory.

Deissler, Oron, and Lee [21] have analyzed the spatial growth of a weakly nonlinear two-dimensional Kuramoto-Sivashinsky equation, which contains an extra translation term, for the evolution of surface waves on a thin film on the outside of a vertical, circular cylinder. The curvature of the cylinder favors two-dimensional waves and they find two-dimensional responses unless the forcing contains significant nonaxisymmetric content.

The objective of the present work is to analyze numerically the Benney equation in two dimensions in a long flow-through domain when the waves are continuously forced by a localized disturbance. If the domain is long enough, one should be able to analyze the wave system fully and compare the behavior with that seen for temporal growth and spatial periodicity. This work then tests the foregoing models and supplies needed information on the behavior of physical systems at small G.

We pose an oscillatory localized disturbance that results in a force parallel to the flow direction and independent of the depth variable. Such a force might be realized by applying a body force in the x direction by, for example, a local thermal gradient, which in turn creates either a local buoyancy gradient or a local variation in viscosity or both (assuming that thermocapillary forces are negligible). We derive a generalized Benney equation for this case leading to an inhomogeneous evolution equation. We numerically integrate this equation for films on a vertical plate for fixed forcing frequencies ω, describe the behavior obtained, and compare this with results of the two-dimensional temporal theory.

II. FORMULATION

Consider a two-dimensional viscous falling film on a vertical plate. The fluid is Newtonian and of constant density. The gas-liquid interface has a surface tension σ and the gas bounding the interface is considered passive.

Let the positive x and z directions be given by the flow direction and normal to the plate into the liquid, respectively. All quantities are taken to be independent of y.

In a fixed neighborhood in space, a force is applied to the liquid-gas interface in the flow direction, given by F. It is localized in space and periodic in time t. Let us denote the effective nondimensional wave number of the response in the x direction by

$$\epsilon=\frac{2\pi h_0}{\lambda}, \tag{1}$$

where h_0 is the mean depth of the film and λ is the effective wavelength. The now-standard long-wavelength approximation is made, $\epsilon\ll 1$, and the dependent variables are developed in powers of ϵ. If $z=h(x,t)$ and the interface shape is unknown for the moment, it is straightforward to show that

$$u\sim G(h\zeta-\tfrac{1}{2}\zeta^2)+\epsilon\{p_{0\xi}(\tfrac{1}{2}\zeta^2-h\zeta)+\tfrac{1}{6}G^2(\tfrac{1}{4}h\zeta^4-h^4\zeta) + Gh_\tau(\tfrac{1}{6}\zeta^3-\tfrac{1}{2}h^2\zeta)+F(\xi,\tau)(h\zeta-\tfrac{1}{2}\zeta^2)\}, \tag{2}$$

$$w\sim-\epsilon\tfrac{1}{2}Gh_\xi\zeta^2-\epsilon^2[\tfrac{1}{2}p_{0\xi\xi}(\tfrac{1}{3}\zeta^3-h\zeta)-p_{0\xi}h_\xi\zeta^2 + \tfrac{1}{12}G^2(hh_\xi)_\xi(\tfrac{1}{10}\zeta^5-h^3\zeta^2)-\tfrac{1}{4}G^2h^3h_\xi^2\zeta^2 + \tfrac{1}{4}Gh_{\tau\xi}(\tfrac{1}{6}\zeta^4-h^2\zeta^2)-\tfrac{1}{2}Ghh_\tau h_\xi\zeta^2 + \tfrac{1}{2}F_\xi(\xi,\tau)(h\zeta^2-\tfrac{1}{3}\zeta^3)+\tfrac{1}{2}F(\xi,\tau)h_\xi\zeta^2], \tag{3}$$

where ξ, ζ, and τ are the x and z coordinates, time scaled on h_0, ϵh_0, and $\epsilon h_0/U_s$, respectively, and u is scaled by the velocity at the surface $U_s=gh_0^2/\nu$; ν is the kinematic viscosity of the fluid. The pressure p is scaled on $\rho\nu U_s/h_0$ and ρ is the density of the fluid.

If Eqs. (2) and (3) are substituted into the kinematic boundary condition, one obtains, for two-dimensional flows, an inhomogeneous Benney equation

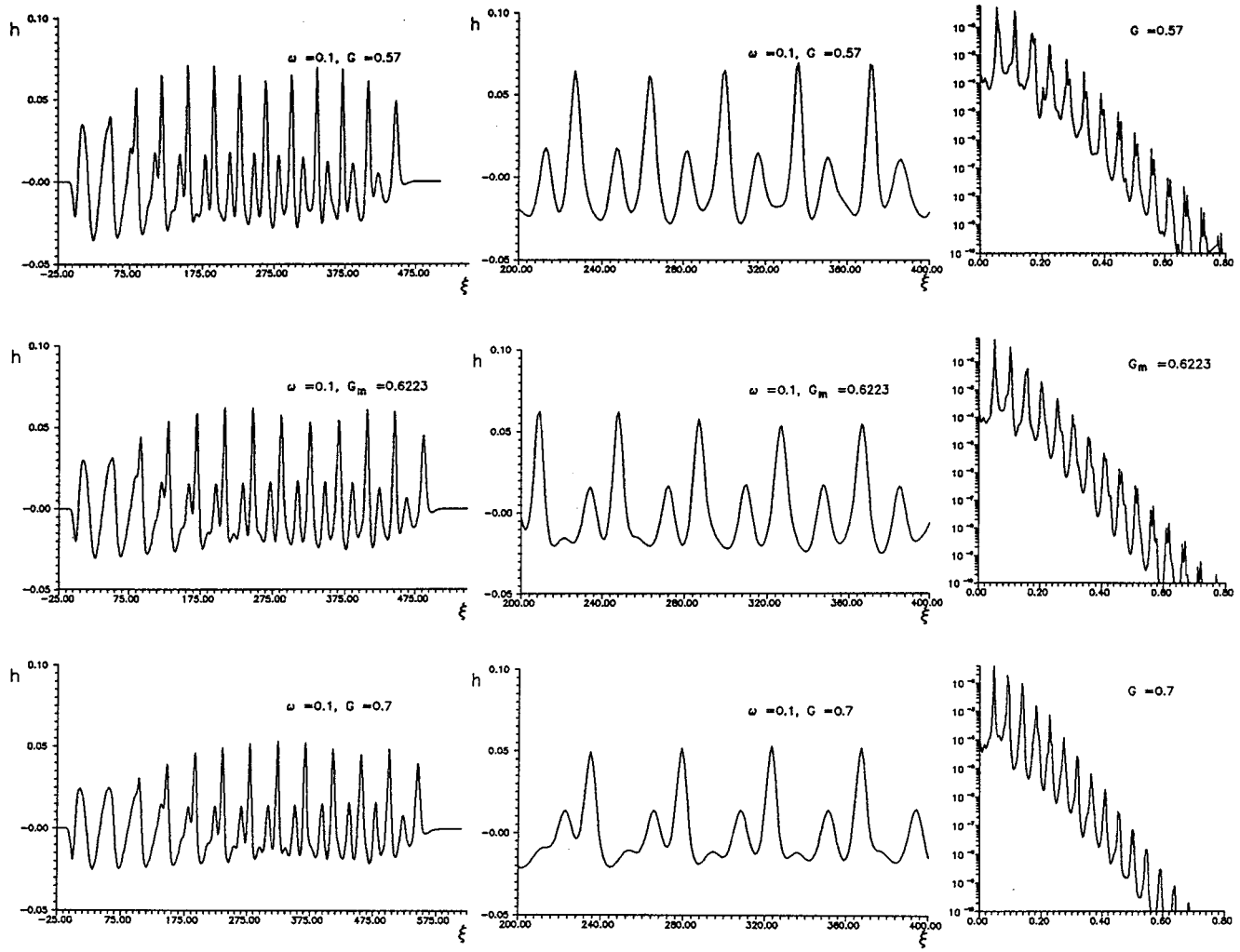

(a)

FIG. 3. (a) Wave profiles for $\omega = 0.1$ in the supercritical region. The first column is the profile shown in the spatial range reached in the time τ shown for the corresponding G. The second column shows an interesting section of the spatial range. The third column shows the power spectrum of the wave measured along the spatial range of the wave. Note that in the figures shown in the third column the abscissa axis represents the spatial frequency, that is, the wavelength. (b) Wave profiles in the subcritical region.

$$h_\tau + Gh^2 h_\xi + \epsilon[\tfrac{2}{15}G^2 h^6 h_\xi + \overline{S}h^3 h_{\xi\xi\xi}]_\xi = -\tfrac{1}{3}\epsilon[F(\xi,\tau)h^3]_\xi. \tag{4}$$

Here we have used the relation

$$p_0 = -3\overline{S}h_{\xi\xi} \tag{5}$$

and

$$G = \frac{gh_0^3}{\nu^2}, \tag{6}$$

$$\overline{S} = \epsilon^2 \frac{\sigma}{3\rho\nu^2}. \tag{7}$$

This equation is the starting point of our study. Equation (4) will be solved numerically on a box of length $l = L/h_0$ (see Fig. 1); the interface is pinned at each end and forced by F at a station upstream of the region of interest. We shall use

$$F(\xi,\tau) = Ae^{-a\xi^2}\sin\omega\tau, \tag{8}$$

where A, $a > 0$, L, and ω are chosen for various cases.

Consider first the linearized, inhomogeneous equation obtained from Eq. (4) by linearizing about $\zeta = 1$,

$$h'_\tau + Gh'_\xi + \epsilon[\tfrac{2}{15}G^2 h'_\xi + \overline{S}h'_{\xi\xi\xi}]_\xi = -\tfrac{1}{3}\epsilon[F(\xi,\tau)]_\xi. \tag{9}$$

After normal modes $\exp(i\omega\tau)$ are inserted in Eq. (9), the code SUPORT [22] is used to solve the resulting ordinary differential equation on a ξ interval, where the left-hand boundary is chosen in order to be clear of the forcing. The boundary conditions used were $h' = h'_\xi = 0$ at both ends of the ξ interval. The values of the fixed parameters are $\overline{S} = 1$ and $\epsilon = 0.01$.

It was found that the Gaster transformation [23] relating spatial and temporal growth is satisfied, i.e., $\Gamma_S = -(\partial\omega/\partial k)^{-1}\Gamma_T$, where the Γ are the growth rates and k is the wave number. In the present case,

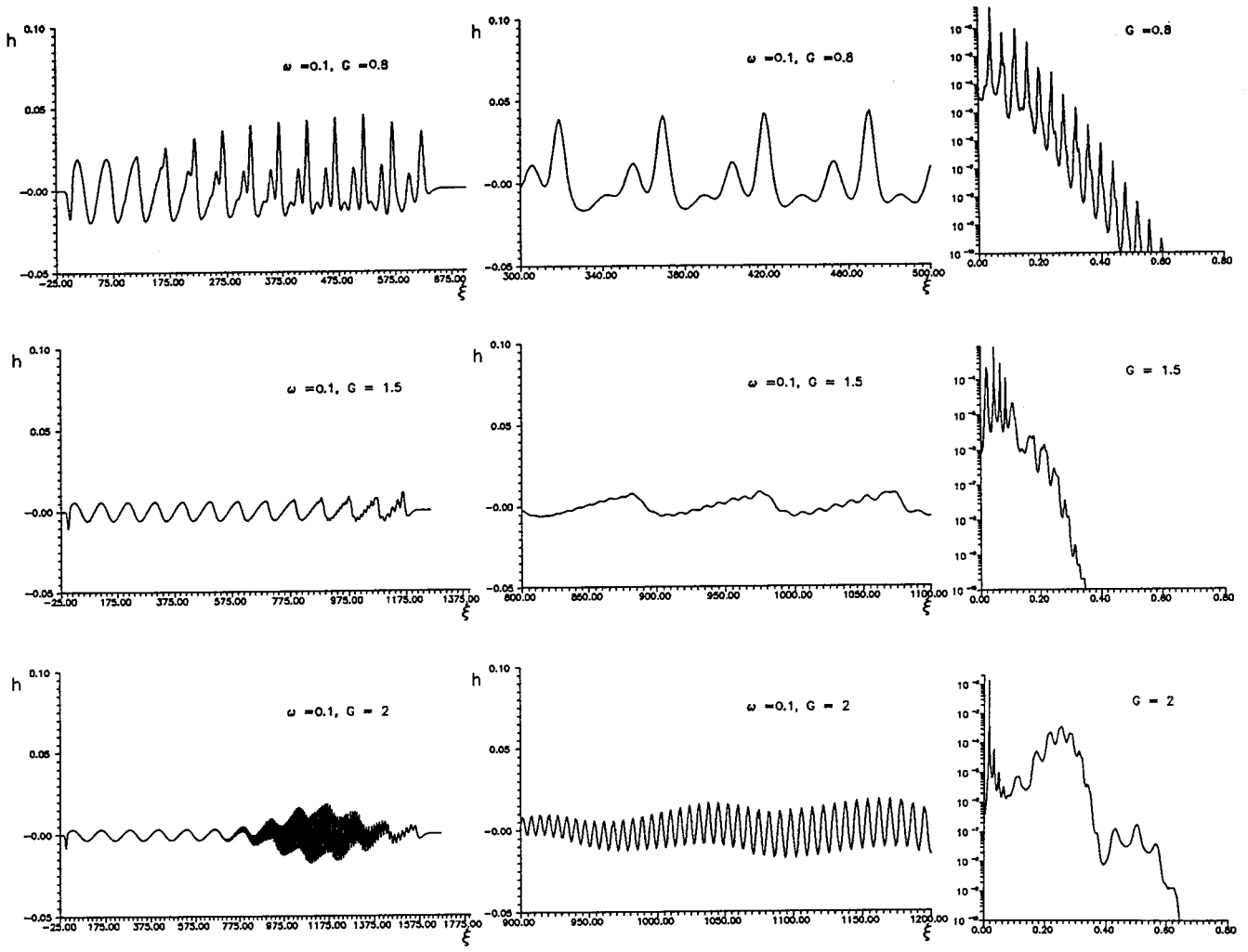

(b)

FIG. 3. (*Continued*).

$$\Gamma_T = \epsilon k^2 [\tfrac{2}{15} G^2 - k^2 \overline{S}] . \tag{10}$$

Further, the amplitude decreases with frequency while the critical Reynolds number increases.

The time evolution of the Benney equation has been investigated by Gjevik [6], who studied the nonlinear interaction of spatially periodic, two-dimensional perturbations. A Fourier expansion of the interface shape was truncated at three terms and gave three coupled ordinary differential equations for h. He showed that the k-G plane contains two curves: a neutral curve k_c versus G and a transition curve k_s versus G, as shown in Fig. 2. Above the neutral curve, infinitesimal perturbations decay. Below this curve, such disturbances grow with time and are predicted to equilibrate to finite-amplitude traveling waves. Below the transition curve, the growing disturbances do not equilibrate. These instability regions correspond to supercritical and subcritical bifurcations, respectively.

From Eq. (10), the cutoff wave number is

$$k_c^2 = \frac{2}{15} \frac{G^2}{\overline{S}}. \tag{11}$$

The wave number corresponding to the maximum growth rate is k_m and the transition curve is at k_s [6], where

$$k_c^2 = 4k_s^2 = 2k_m^2 , \tag{12}$$

as shown in Fig. 2.

The numerical solution of Eq. (4) is made in a spatial interval taken to be ξ between -100 and $100 + G\tau$, as shown in Fig. 1, where τ is the time required for waves to propagate a predetermined distance. The forcing is near $\xi = 0$ and at both ends the interface is pinned, $h = h_\xi = 0$. The initial conditions are $h = h_\xi = 0$ at $\tau = 0$. Equation (4) is numerically integrated by means of finite differences in space and time, keeping $G\Delta\tau/(\Delta\xi)^2 < 0.01$.

III. RESULTS AND DISCUSSION

In Figs. 3 and 4 to follow, the left-hand column indicates the spatial variations in h at fixed times, the middle column an amplified picture of a region of interest, and the third column a power spectrum of the whole record at a fixed time. As the row number increases, so does the Reynolds number G. Figures 3(a) and 4(a) show results of the evolu-

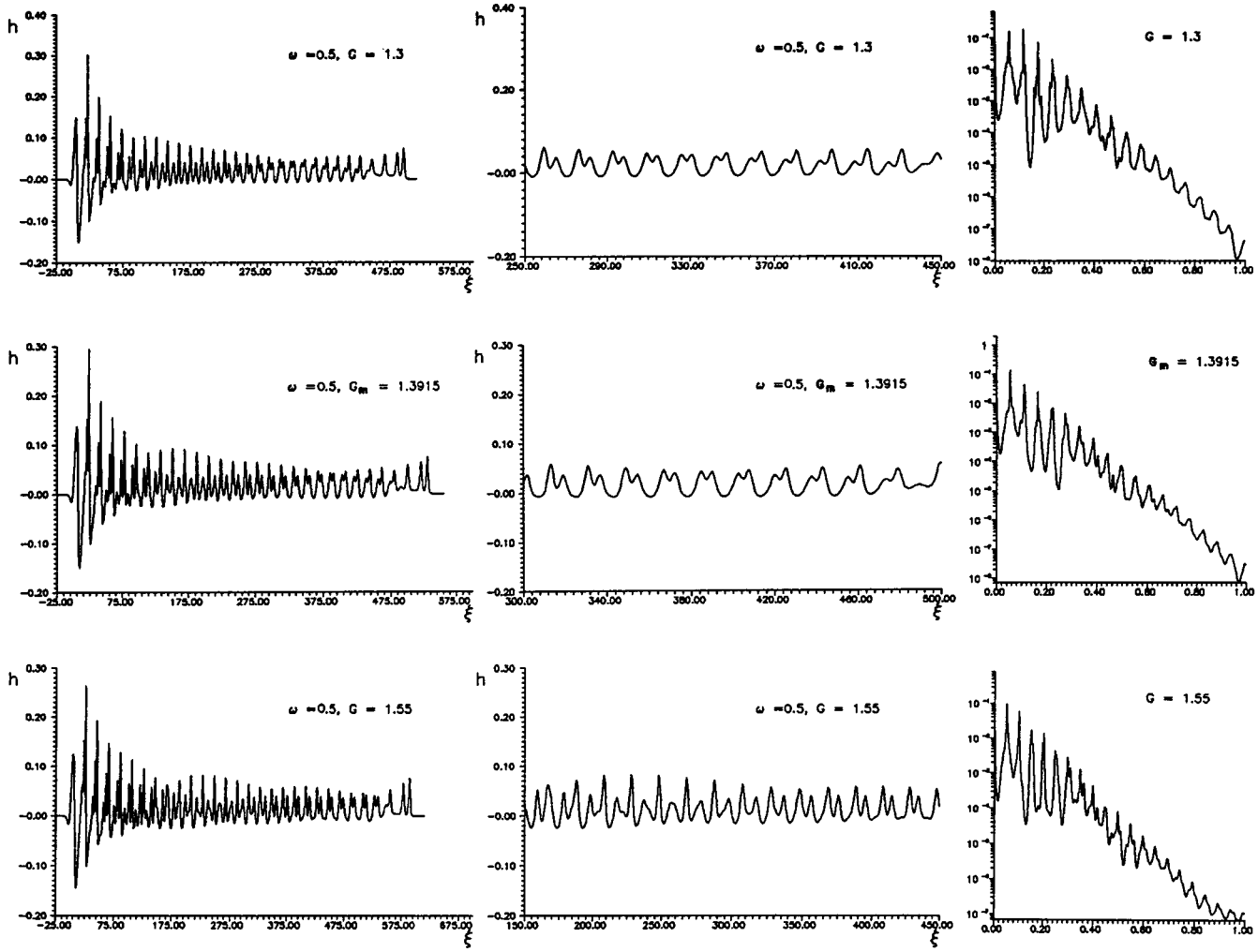

(a)

FIG. 4. (a) Wave profiles for $\omega = 0.5$ in the supercritical region. (b) Wave profiles in the subcritical region.

tion for $k_s<k<k_c$, where in temporal nonlinear theory, disturbances equilibrate to finite-amplitude traveling waves. Figures 3(b) and 4(b) show the results at corresponding points of operation for $k<k_s$, where temporal theory gives unbounded growth according to the homogeneous Benney equation. All the operating points are indicated in Fig. 2. In all the calculations presented below, $\epsilon=0.01$, $S=1.0$, $A=0.005$, and $a=0.05$.

Before presenting the details of the results, we summarize the overall findings. In Fig. 2 the dots represent parameter values where the spatial integration yields equilibrated nonlinear states. The crosses locate parameter values where the generalized Benney equation predicts blowup (though the physical system would not necessarily display this behavior).

One sees that up to a value ω_c, between 1.0 and 1.5, the spatial growth case parallels the temporal growth case in that the equilibrated states occur for $k_s<k<k_c$. Above ω_c, ω is so large that in this region the evolution equation sometimes or always predicts blowup. The states can be pure harmonic waves or waves with two or more basic frequencies. The harmonics will appear as the Reynolds number increases. For small frequencies the harmonics appear for $k<k_s$, but as ω is increased, harmonics will appear in $k_s<k<k_c$. The number of harmonics increases with G until irregular behavior is seen. Modulation of the waves is found for $k< k_s$ and for all G up to $\omega=1$. However, an increase of ω prevents observable modulation for G just below linear criticality at $\omega=1.5$, for $G\leqslant 2.603$ at $\omega=1.75$, etc. In this initial study, only vertical films are considered and no attempt has been made to test the sensitivity of the results to changes in the forcing (parameters A and a) or material properties (parameter S).

Figure 3(a) shows the wave at time $t=800$ in the region between k_c and k_s as G increases from 0.57 to 0.70 where $G_m=0.6223$. The first case is close to k_c and the third is very close to and above k_s. Here it is easy to observe the nonlinear evolution. The crests saturate into a modulated wave with two or three harmonics, as shown clearly for $G=0.7$. Note that as G increases the wavelengths of both the principal wave and the modulation wave increase. Figure 3(b) shows results at $k< k_s$. For $G=0.8$ it is shown that the harmonics and the modulation of the wave appear further downstream than before. For $G=0.8$ the wave still saturates and the harmonics are well defined. As G is increased to 1.5 a larger number of harmonics appear and the power spectrum shows

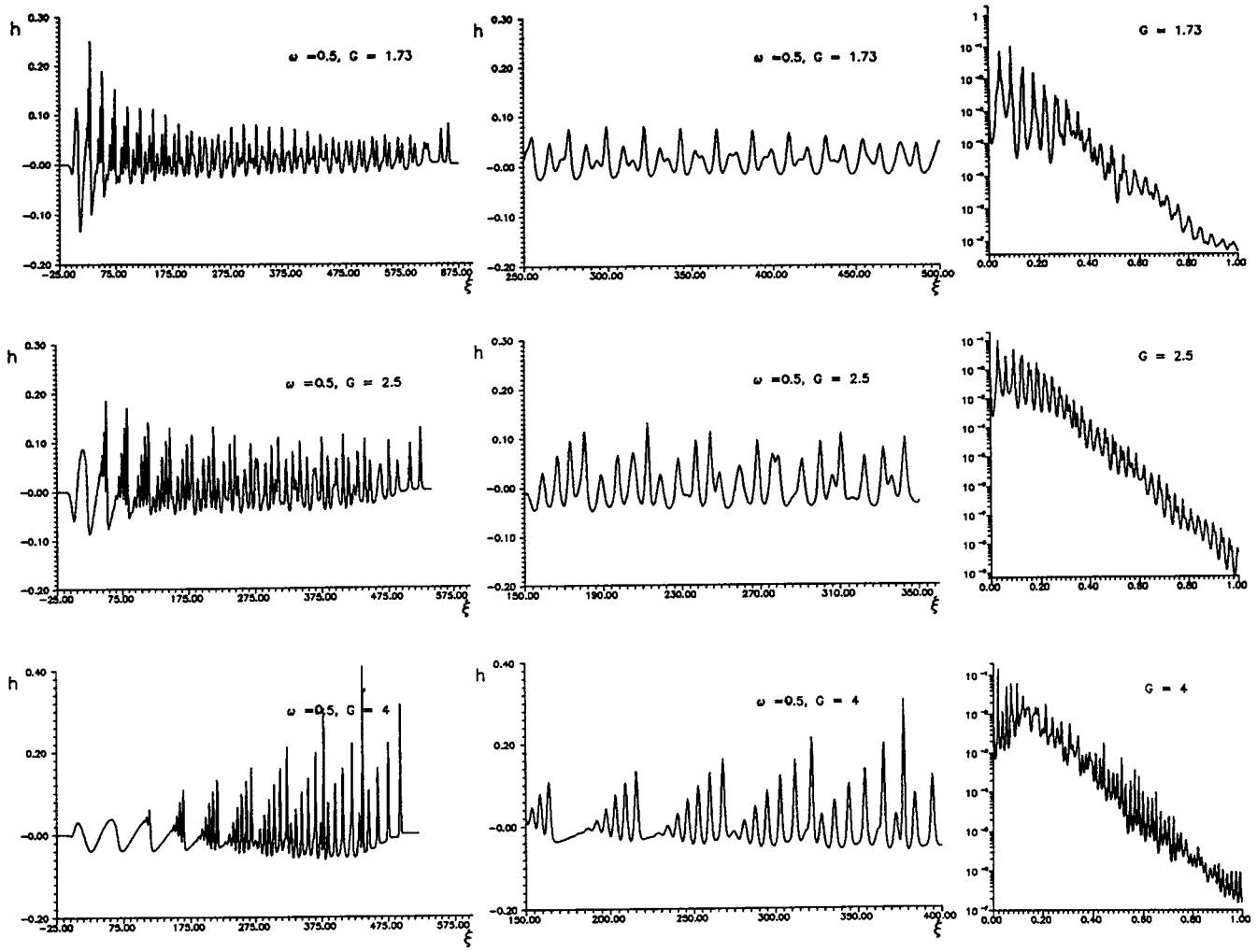

(b)

FIG. 4. (*Continued*).

a broadband section. When G is increased to 2.0, a great number of harmonics appear, the flow becomes irregular after some distance from the origin, and the power spectrum shows a broadband structure.

Note that in all the graphs of Fig. 3 the wave crests without harmonics occupy a longer distance from the origin as the Reynolds number increases and, at the same time, due to the nonlinear evolution the number of wave harmonics increases. This is due to the dual role played by G, since it is simultaneously both the phase velocity and the flow rate.

Figures 4(a) and 4(b) correspond to $\omega=0.5$. Figure 4(a) corresponds to waves in the range $G = 1.3$, near k_c, to $G=1.55$, near k_s. Here $G_m=1.3915$. The time is set to 360 units and the last snapshot of the wave is presented. At this frequency, two harmonics appear just below k_c, but just above k_s we do not find three harmonics, as in the case of Fig. 3(a). The early perturbations in the three pictures are very large compared to that of the equilibration because the nonlinear region appears immediately at such high frequency of oscillation and due to the relatively small phase speed. There is again wave modulation, but it is not easy to see for $G=1.3$. Modulation is easy to recognize for large Reynolds numbers, as in the other wave profiles of Figs. 4(a) and 4(b).

In Fig. 4(b) it is shown that three harmonics appear just below k_s when $G=1.73$. This wave profile still shows saturation. For $G=2.5$ there are still three harmonics, but after some time its amplitude grows so fast that saturation is not attained. Therefore, the wave profile is presented only for $\tau=200$. For $G=4$ six harmonics appear, but the growth rate is so large that only the wave for $\tau=120$ is given. The power spectrum for the wave with $G=4$ is a broadband spectrum that shows its chaotic structure.

For larger flow rate and frequency blowup might be eventually expected since the basic assumptions of small inertial effects and of surface slopes will, at some point in space or time, be violated. One must resort, then, to direct numerical solution of the governing equations. Additional figures showing the wave development for longer times and higher frequencies and its development in time at two fixed points in space are given by Dávalos-Orozco *et al.* [24]; see also Dávalos-Orozco *et al.* [25].

IV. CONCLUSION

In this paper we investigated the two-dimensional stability of a fluid layer flowing down a vertical plate. The analy-

sis is based on an inhomogeneous Benney equation (IBE) in which the inhomogeneous term represents the forcing due to a steadily oscillating localized surface shear stress. Through that term, the flow is controlled by the frequency of oscillation ω. This equation is investigated in the parameter plane (k,G) divided in three main regions of stability $k_c<k$, supercriticality $k_s<k<k_c$ and subcriticality $k<k_s$.

The results presented in this paper show that the time of validity of the IBE depends on the imposed frequency and the Reynolds number. It is shown that, for any frequency of oscillation, above a critical G the numerical solution blows up after some time which is shorter when G was larger. For small frequencies this behavior arose for $k<k_s$. However, for frequencies above a critical one, ω_c, nonsaturating behavior was also found inside the supercritical region $k_s<k<k_c$.

The nonsaturating behavior is unphysical, but gives the limitations on the magnitudes of the parameters involved in the problem.

We also found evidence that irregular behavior before blowup occurred. It is possible that this behavior can appear in the experiment in the same parameter range as predicted by the IBE. In a recent paper Liu and Gollub [20] obtained experimental results for very small angle of inclination of the plate in order to understand the mechanism leading to the transition to spatio-temporal chaos. They concluded that sideband and subharmonic instabilities, which occur at high and low frequencies, respectively, are involved in the transition to chaos.

As shown in our numerical results, an increase in G leads to an increase in the number of harmonics. Therefore, due to their mutual nonlinear interaction, some of the above mentioned mechanisms may lead in time and space to the chaotic behavior observed.

ACKNOWLEDGMENTS

L.A.D.-O. appreciates support from DGAPA-UNAM under Project No. IN104094. This work was partially supported by the U.S. Department of Energy, Basic Energy Sciences Program.

[1] T. R. Salamon, R. C. Armstrong, and R. A. Brown, Phys. Fluids **6**, 2202 (1994).
[2] S. Krisnamoorthy, B. Ramaswamy, and S. W. Joo, Phys. Fluids **7**, 2291 (1995).
[3] S. W. Joo and S. H. Davis, J. Fluid Mech. **242**, 529 (1992).
[4] A. L. Frenkel, Phys. Fluids A **5**, 2342 (1993).
[5] D. J. Benney, J. Math. Phys. **45**, 150 (1966).
[6] B. Gjevik, Phys. Fluids **13**, 1918 (1970).
[7] C. Nakaya, Phys. Fluids **18**, 1407 (1975).
[8] M. V. G. Krishna and S.-P. Lin, Phys. Fluids **20**, 1039 (1977).
[9] A. Pumir, P. Manneville, and Y. Pomeau, J. Fluid Mech. **135**, 27 (1983).
[10] H.-C. Chang, Phys. Fluids A **1**, 1314 (1989).
[11] C. Nakaya, Phys. Fluids A **1**, 1143 (1989).
[12] S. W. Joo, S. H. Davis, and S. G. Bankoff, J. Fluid Mech. **230**, 117 (1991).
[13] S. W. Joo, S. H. Davis, and S. G. Bankoff, Phys. Fluids A **3**, 231 (1991).
[14] S. W. Joo and S. H. Davis, Chem. Eng. Commun. **118**, 111 (1992).
[15] S. W. Joo, S. H. Davis, and S. G. Bankoff, Nucl. Eng. Design **141**, 225 (1993).
[16] G. I. Sivashinsky and D. M. Michelson, Prog. Theor. Phys. **63**, 2112 (1980).
[17] S.-P. Lin and C.-Y. Wang, in *Encyclopedia of Fluid Mechanics*, edited by N. P. Cheremisionoff (Gulf, Houston, TX, 1985), Vol. 1, pp. 931–951.
[18] D. M. Maron, N. Brauner, and A. Dukler, Phys. Chem. Hydrodyn. **6**, 87 (1985).
[19] M. Cheng and H.-C. Chang, Phys. Fluids **7**, 34 (1994).
[20] J. Liu and J. P. Gollub, Phys. Rev. Lett. **70**, 2289 (1993).
[21] R. J. Deissler, A. Oron, and Y.-C. Lee, Phys. Rev. A **43**, 4558 (1991).
[22] M. R. Scott and H. A. Watts, SIAM J. Numer. Anal. **14**, 40 (1977).
[23] M. Gaster, J. Fluid Mech. **14**, 222 (1962).
[24] L. A. Dávalos-Orozco, S. H. Davis, and S. G. Bankoff, Technical Northwestern University Report No. 9505, 1996 (unpublished).
[25] L. A. Dávalos-Orozco, S. H. Davis, and S. G. Bankoff, in *International Union of Theoretical and Applied Mechanics Symposium on Waves in Liquid/Vapour Two-Phase Systems*, edited by S. Morioka and L. Wijngaarden (Kluwer Academic, Dordrecht, Netherlands, 1995), p. 225.